

TRANSVERSE COUPLED-BUNCH INSTABILITIES IN DAMPING RINGS OF HIGH-ENERGY LINEAR COLLIDERS*

K.A. THOMPSON AND R.D. RUTH

Stanford Linear Accelerator Center

Stanford University, Stanford, California 94305

ABSTRACT

In this paper we present methods for studying and controlling transverse coupled bunch instabilities. Our primary motivation is the study of damping rings for next-generation linear colliders in which many bunches are damped in the same ring simultaneously, however, the methods presented are also applicable to other situations. The theory developed here treats the motion of the bunch centroids, since the coherent dipole modes of coupled-bunch oscillation are expected to be strongly dominant. A formalism to obtain the n normal modes of oscillation of n bunches is developed. The imaginary part of the frequency of each normal mode determines its stability. However, not only the long term stability of each oscillation mode, but also the transient behavior of the bunches just after injection must be considered in damping rings. Two methods of studying the transient behavior are presented: (1) A Laplace transform method, using the eigenmodes and corresponding eigenfrequencies found by the normal modes formalism, and (2) computer tracking, using a localized-kick approximation. Examples are given for damping ring designs appropriate to a linear collider of about 0.5 to 1.0 TeV center of mass energy.

Submitted to *Physical Review D*.

† Work supported by the Department of Energy, contract DE-AC03-76SF00515.

TRANSVERSE COUPLED-BUNCH INSTABILITIES IN DAMPING RINGS OF HIGH-ENERGY LINEAR COLLIDERS*

K.A. THOMPSON AND R.D. RUTH

Stanford Linear Accelerator Center

Stanford University, Stanford, California 94305

ABSTRACT

In this paper we present methods for studying and controlling transverse coupled bunch instabilities. Our primary motivation is the study of damping rings for next-generation linear colliders in which many bunches are damped in the same ring simultaneously, however, the methods presented are also applicable to other situations. The theory developed here treats the motion of the bunch centroids, since the coherent dipole modes of coupled-bunch oscillation are expected to be strongly dominant. A formalism to obtain the n normal modes of oscillation of n bunches is developed. The imaginary part of the frequency of each normal mode determines its stability. However, not only the long term stability of each oscillation mode, but also the transient behavior of the bunches just after injection must be considered in damping rings. Two methods of studying the transient behavior are presented: (1) A Laplace transform method, using the eigenmodes and corresponding eigenfrequencies found by the normal modes formalism, and (2) computer tracking, using a localized-kick approximation. Examples are given for damping ring designs appropriate to a linear collider of about 0.5 to 1.0 TeV center of mass energy.

† Work supported by the Department of Energy, contract DE-AC03-76SF00515.

TRANSVERSE COUPLED-BUNCH INSTABILITIES IN DAMPING RINGS OF HIGH-ENERGY LINEAR COLLIDERS

K.A. THOMPSON AND R.D. RUTH

Stanford Linear Accelerator Center

Stanford University, Stanford, California 94305

+1pt-1pt

ABSTRACT

In this paper we present methods for studying and controlling transverse coupled bunch instabilities. Our primary motivation is the study of damping rings for next-generation linear colliders in which many bunches are damped in the same ring simultaneously, however, the methods presented are also applicable to other situations. The theory developed here treats the motion of the bunch centroids, since the coherent dipole modes of coupled-bunch oscillation are expected to be strongly dominant. A formalism to obtain the n normal modes of oscillation of n bunches is developed. The imaginary part of the frequency of each normal mode determines its stability. However, not only the long term stability of each oscillation mode, but also the transient behavior of the bunches just after injection must be considered in damping rings. Two methods of studying the transient behavior are presented: (1) A Laplace transform method, using the eigenmodes and corresponding eigenfrequencies found by the normal modes formalism, and (2) computer tracking, using a localized-kick approximation. Examples are given for damping ring designs appropriate to a linear collider of about 0.5 to 1.0 TeV center of mass energy.

1. INTRODUCTION

In this paper we present methods for studying transverse coupled-bunch instabilities, for the case in which the bunches are not necessarily spaced equally on the circumference of the ring, and in which the wakefields may be of quite general form. The major motivation for this work is the study of such instabilities in damping rings for a next-generation (~ 1 TeV center of mass energy) linear collider.¹ In order to maximize the luminosity and the energy efficiency, it is desirable to accelerate a train of bunches on each rf fill of the linacs, rather than just a single bunch. If this is to be feasible, then multibunch instabilities must be controlled in all subsystems of the collider; the transverse instability in the main linacs is potentially very severe and has been addressed elsewhere.² It is envisioned that the damping rings of the collider will contain several bunch trains at a time, to allow a higher repetition rate (where "repetition rate" denotes the number of rf fills per unit time). At a given time, the damping ring is to contain several such trains (~ 10), each at a different stage of damping; on each rf fill, the "oldest" train gets extracted for acceleration to high energy in the linac of the collider.

The bunches within a train are rather closely spaced (typically 1-2 rf wavelengths at a damping ring rf frequency of 1.4 GHz); thus, the bunches toward the end of a train are strongly affected by the wakefields from the preceding bunches. While the trains themselves may be separated by many rf wavelengths, they can still affect each other through long-range wakefields, unless these wakefields are very heavily damped.

Our formalism can also be used to study the coupled-bunch instabilities of either of the two oppositely-circulating beams in a storage ring. There are, of course, well-known methods for calculating the growth rates of the n normal modes of coupled oscillation of n symmetrically placed bunches.³⁻⁵ Although the emphasis of

the present paper will be on damping rings containing bunches clumped into several trains, in the storage ring case there is also a motivation for using the present formalism, since it is sometimes desirable to operate storage rings with gaps in the bunch pattern, for example, to counteract the build-up of ions. Using the techniques presented here, one may study the stability of various strategies for injection or extraction of intense trains of bunches from any ring, whether it be used for colliding beams or for damping beams to be injected into a linear collider. Indeed, coupled bunch instabilities and their transient behavior are important considerations in the design of the new generation of heavy quark factories. Application of our formalism to such a case has been discussed elsewhere.⁶

We present a semi-analytic, normal-modes approach, in which the bunches need not be symmetrically placed on the circumference. The focusing forces due to the ring lattice are represented by a smooth focusing approximation. As the bunches circulate in the ring, they excite currents in components of the vacuum chamber, which can in turn produce fields that act back on the bunches. These forces can be expressed in terms of a wakefield. The form of the wakefield can be quite arbitrary, for example, sums of resonant modes in rf cavities or other structures, and/or the resistive wall wake. The problem of finding the coherent frequencies and oscillation modes amounts to finding the eigenvalues and eigenvectors of a matrix; the elements of the matrix are derived analytically for the wakefields of interest. It is then straightforward to solve for the eigenvalues and eigenvectors numerically. The sign of the imaginary part of each eigenvalue determines the stability of the corresponding normal mode of oscillation.

Even if there is sufficient damping present that all the normal modes of oscillation are stable, interference between modes can produce transient blow-up of the beam. This transient behavior can be important in damping rings since the storage times

are short. In addition, for sufficiently strong wakes and long trains of bunches, the transient could be large enough to cause beam loss at injection. Thus, it is desirable to be able to calculate the motion of each bunch as a function of time, given the initial conditions of all the bunches. We have developed two independent methods of studying this transient behavior:

1. Given the coherent frequencies and normal modes, the Laplace transform can be used to obtain the motion of the bunches, taking the initial conditions into account.
2. One may use a computer tracking method to obtain the offset of each bunch as a function of time. This is straightforward and computationally efficient provided that the number of bunches is not too large and the wakefields do not persist for too many turns.

The case of strongly damped wakefields is readily handled by the tracking method, since the wakes are negligible after few turns. Cases with long-range wakefields are most efficiently handled by the Laplace transform method. For a wide range of intermediate situations, both methods are applicable and give the same results.

Note that in our analysis, we shall ignore any coupling between the two transverse directions. This is reasonable since for the damping ring design of interest here, coupling of the vertical and horizontal directions is kept small in order to maintain a very flat beam. We also ignore coupling between the transverse and longitudinal directions, which is justified since resonances can be avoided by choosing the synchrotron and betatron frequencies appropriately.

2. EQUATIONS OF TRANSVERSE MOTION

In this section we review some necessary definitions and obtain the equations governing the coherent transverse motion of the bunches circulating in a damping ring or other storage ring. By *coherent motion* we mean the motion of the centroid of each bunch; the equations of motion will be those of bunches each consisting of a single macroparticle. The internal “incoherent” motion of the particles making up the bunches is taken into account only when necessary, i.e. in the computation of the damping parameters that will appear in these equations of motion.

We begin by considering a single particle moving in a focusing lattice. The equation of motion for the transverse displacement $x(s)$ of the particle is

$$x'' + K(s)x(s) = 0 \quad , \quad (2.1)$$

where $K(s)$ represents the strength of the focusing lattice as a function of longitudinal coordinate s along the circumference. Here primes represent derivatives with respect to s . Clearly $K(s)$ is periodic in s , that is,

$$K(s + C) = K(s) \quad , \quad (2.2)$$

where C is the circumference of the ring. Solutions to the homogeneous equation (2.1) may be written

$$x(s) = \beta(s)^{1/2} \cos[\phi(s) + \phi_0] \quad , \quad (2.3)$$

where the Courant-Snyder *beta function* $\beta(s)$ satisfies⁷

$$\frac{1}{2}\beta\beta'' - \frac{1}{4}(\beta')^2 + K(s)\beta^2 = 1 \quad , \quad (2.4)$$

and the phase advance $\phi(s)$ from some reference point $s = 0$ is defined by

$$\phi(s) \equiv \int_0^s \frac{ds}{\beta(s)} \quad (2.5)$$

The *betatron tune* of the ring is defined to be the total number of betatron oscillations around the ring:

$$\nu \equiv \frac{1}{2\pi} \oint \frac{ds}{\beta(s)} \quad (2.6)$$

The *transfer matrix* relates the values of (x, x') for a particle undergoing pure betatron motion, *i.e.*, satisfying Eq. (2.1), between two points s_1 and s_2 in the ring:

$$\begin{pmatrix} x(s_2) \\ x'(s_2) \end{pmatrix} = \mathbf{M} \begin{pmatrix} x(s_1) \\ x'(s_1) \end{pmatrix} \quad (2.7)$$

Using Eq. (2.3), \mathbf{M} is found to be

$$\mathbf{M} = \begin{pmatrix} \left(\frac{\beta_2}{\beta_1}\right)^{1/2}(\cos \phi_{12} + \alpha_1 \sin \phi_{12}) & (\beta_1 \beta_2)^{1/2} \sin \phi_{12} \\ \frac{(\alpha_1 - \alpha_2) \cos \phi_{12} - (1 + \alpha_1 \alpha_2) \sin \phi_{12}}{(\beta_1 \beta_2)^{1/2}} & \left(\frac{\beta_1}{\beta_2}\right)^{1/2}(\cos \phi_{12} - \alpha_2 \sin \phi_{12}) \end{pmatrix} \quad (2.8)$$

Here $\beta_i \equiv \beta(s_i)$, $\alpha_i = \alpha(s_i)$ where $\alpha(s) \equiv -\frac{1}{2}\beta'(s)$, and $\phi_{12} \equiv \int_{s_1}^{s_2} \frac{ds}{\beta(s)}$ is the betatron phase shift between the two points.

The quantity

$$J \equiv \frac{1}{2\beta} \left[x^2 + \left(\beta x' - \frac{\beta' x}{2} \right)^2 \right] \quad (2.9)$$

is readily shown to be an invariant for the motion specified by Eq. (2.1), in the absence of synchrotron radiation. At any location on the circumference, $2\pi J$ is equal to the area in the xx' plane enclosed by the ellipse specified by Eq. (2.9), whose coordinates are all the possible values of (x, x') reached by the particle on successive turns. The shape and orientation of the ellipse may change with location on the circumference, but its area is the same at all locations.

A *bunch* consists of many such particles; we define the *emittance* of the bunch to be

$$\epsilon = \langle J \rangle \quad , \quad (2.10)$$

i.e., the average of J over all the particles in the bunch. The normalized emittance $\gamma\epsilon$, where γ is the Lorentz factor $\frac{E}{mc^2}$, is often quoted instead of ϵ , since it remains invariant even when acceleration is present. In referring to a bunch, the transverse offset x is of course the offset of the bunch centroid. We assume there are a total of n bunches in the ring, each consisting of N elementary charges e .

We assume the bunches are fully relativistic. Thus, we may equally well use time t in place of s as the independent variable, that is, $s = ct + s_0$. We number the bunches from 1 to n , and denote the spacing between bunches i and j by L_{ij} , taking $L_{ij} > 0$ for $i > j$, and $L_{ij} = -L_{ji}$. It is also convenient to introduce a new variable \bar{s} that has a unique value between 0 and the circumference cT_0 , to make explicit the dependence of location on time for each bunch:

$$\bar{s}_j(t) = ct - L_{j1} - cT_0 \cdot \text{mod}(ct - L_{j1}, cT_0) \quad . \quad (2.11)$$

Here $\text{mod}(a, b)$ denotes the integer part of a/b . Note that we have chosen $\bar{s} = 0$ for bunch 1 at $t = 0$, and that

$$\bar{s}_j(t - \frac{L_{ij}}{c} - qT_0) = \bar{s}_i(t) \quad . \quad (2.12)$$

for any integers i, j , and q .

As each bunch travels through the ring, it excites fields in various components of the vacuum chamber. These fields subsequently act back on other bunches that pass these components. Let us now include this coherent force on the right hand side of

Eq. (2.1). The dominant part of the coherent force affecting the transverse motion can be conveniently expressed in terms of the offsets of the bunch centroids and a transverse *wake function*, using the standard transverse dipole wakefield formalism.^{8,9} The wake function $\mathcal{W}_\perp(z, \bar{s})$ is essentially a Green's function for the interaction between two relativistic bunches via the surrounding vacuum chamber. It depends on z , the separation between the “exciting bunch” (which produces a disturbance at any given location \bar{s}) and the “spectator bunch” (which reaches \bar{s} at the later time z/c). It also depends on the location \bar{s} along the circumference, since the strength of the excitation differs in the various structures (cavities, vacuum chamber, bellows, etc.) present in the ring. The wake function is zero when the argument z is less than or equal to zero, by causality (since the bunches are assumed to be travelling at essentially the speed of light). The transverse dipole wake force acting on a particle of charge e in the spectator bunch is proportional both to the wake function and to the transverse offset that the exciting bunch had when it was at the present location of the spectator bunch. Including the effects of all bunches on all previous turns, the coherent force (per unit mass) on bunch i due to the transverse dipole wake takes the form

$$\begin{aligned}
F(t) &= \frac{Ne^2c^2}{E_0} \sum_{j=1}^n \sum_{q=0}^{\infty} \mathcal{W}_\perp(L_{ij} + qT_0c, \bar{s}_j(t - L_{ij}/c - qT_0)) x_j(t - L_{ij}/c - qT_0) \\
&= \frac{Ne^2c^2}{E_0} \sum_{j=1}^n \sum_{q=0}^{\infty} \mathcal{W}_\perp(L_{ij} + qT_0c, \bar{s}_i(t)) x_j(t - L_{ij}/c - qT_0) \quad .
\end{aligned}
\tag{2.13}$$

Note that $\mathcal{W}_\perp(z, \bar{s})$ is the transverse dipole wake function per unit length, with units $[V/(C \text{ m}^2)]$, and E_0 is the energy of a particle on the design orbit.

Putting everything together and including an exponential damping term, we have for the equation of motion of bunch i :

$$\ddot{\bar{x}}_i(t) + 2\zeta\dot{x}_i(t) + c^2 K(\bar{s}_i(t))x_i(t) = \frac{Ne^2c^2}{E_0} \sum_{j=1}^n \sum_{q=0}^{\infty} \mathcal{W}_{\perp}(L_{ij} + qT_0c, \bar{s}_i(t))x_j(t - L_{ij}/c - qT_0) \quad (2.14)$$

The parameter ζ represents the contributions from all sources of coherent damping of the transverse motion. The computation of ζ requires consideration of the internal structure of the bunches, as will be discussed later. In the general formulation of Eq. (2.14), the focusing function and the wake function both may depend upon location \bar{s} in the ring. We shall make two further simplifying approximations, removing these dependences.

First, we shall replace the beta function $\beta(s)$ with a constant “average” betatron function $\bar{\beta}$. This is reasonable for the damping ring designs to be considered here, since the actual $\beta(s)$ does not depend too strongly on s . The $\bar{\beta}$ is chosen to keep the tune ν the same as in the actual ring, so that

$$\nu = \frac{C}{2\pi\bar{\beta}} = \frac{\omega_{\beta}T_0}{2\pi} \quad , \quad (2.15)$$

thus, from the definition (2.6), $1/\bar{\beta}$ is actually the average around the ring of $1/\beta(s)$. The betatron angular frequency is just $\omega_{\beta} \equiv c/\bar{\beta}$, and $K(\bar{s})$ in Eq. (2.14) is replaced by $(\omega_{\beta}/c)^2$.

Second, although much of the long-range transverse wake force is localized to the rf cavities (and any other high- Q structures), we may treat it as though an averaged force were distributed around the ring, provided that the effect of the transverse wake force on the betatron frequency is small enough. The criterion for obtaining the same result for a localized and a distributed force is that the coherent betatron tune shift due to the wake force be small compared to $\frac{1}{2\pi}$, and that the betatron tune not be near an integer or half-integer resonance. In this case, the coherent tune shift is the

same for a localized wake as it is for the equivalent distributed wake (see Appendix), and thus the corresponding calculations of the coupled-bunch motion give the same result. Thus, we shall make the replacement

$$\mathcal{W}_\perp(L_{ij} + qT_0c, \bar{s}_i(t)) \longrightarrow \frac{W_\perp(L_{ij} + qT_0c)}{cT_0} \quad , \quad (2.16)$$

where

$$W_\perp(z) = \oint \mathcal{W}_\perp(z, \bar{s}) d\bar{s} \quad . \quad (2.17)$$

The units of $W_\perp(z)$ are [V/(C m)].

Thus, our “smoothed” equation of motion for bunch i is

$$\begin{aligned} \ddot{x}_i(t) + 2\zeta\dot{x}_i(t) + \omega_\beta^2 x_i(t) = \\ \frac{Ne^2c}{E_0T_0} \sum_{j=1}^n \sum_{q=0}^{\infty} W_\perp(L_{ij} + qT_0c) x_j(t - qT_0 - L_{ij}/c) \quad . \end{aligned} \quad (2.18)$$

As an aside, we note that if the betatron function were to vary strongly with location \bar{s} , then this would not necessarily be a good approximation, since the effect of $\mathcal{W}_\perp(z, \bar{s})$ will be enhanced when the local value of the beta function, $\beta(\bar{s})$, is large.

Alternatively, we may go to the other extreme of a localized kick approximation, as will be discussed later in the section on tracking. Both formulations give the same result in the regime of interest here, where the change in betatron tune due to the wakefield is small.

The set of all $x_i(t)$ gives a “snapshot” of all the bunch positions at time t . Another convention that is sometimes useful is to interpret time t to have a different fixed offset for each bunch, such that each bunch passes some reference location (for instance, the injection point) at $t = 0$. In this case, one should take $x_j(t - qT_0)$ in place of $x_j(t - qT_0 - L_{ij}/c)$ in Eq. (2.18), in which case the time variable for bunch i runs

L_{i1}/c behind the time variable for bunch 1 — this is merely an incorporation of the difference in the spatial positions of the bunches into their time coordinates.

3. EXPLICIT FORMS OF THE WAKE FUNCTION

Before proceeding further, we give in this section the explicit expressions for the transverse dipole wake functions $W_{\perp}(z)$ of important ring components (Refs. 5 and 8).

3.1. RESONANT STRUCTURE

The transverse dipole wake function of a resonant structure may be written as a sum of modes of the form:

$$W_{\perp}(z) = \begin{cases} \sum_m \frac{W_m}{2i} [e^{ik_m z} - e^{-ik_m^* z}] & (z > 0) \\ 0 & (z < 0) \end{cases} \quad (3.1)$$

where the W_m are constants, and the k_m are allowed to be complex to take damping of the modes into account. Clearly, each mode is a damped sine. The wake function may be calculated numerically for resonant structures, using one of a number of existing computer codes, for example, URMEL¹⁰ or TRANSVRS.¹¹

Note that since the bunches have a finite length, there is a cutoff for wakefield modes of sufficiently high frequency. For Gaussian bunches of rms length σ_z , the cutoff factor is $e^{-k_m^2 \sigma_z^2}$; we assume such factors are absorbed into the coefficients W_m .

3.2. RESISTIVE WALL

The transverse dipole resistive wall wake function may be written¹²

$$W_{\perp}(z) = \frac{2L_w}{\pi b^3} \left(\frac{c}{4\pi\epsilon_0\sigma} \right)^{1/2} z^{-1/2} . \quad (3.2)$$

This is a wake per unit length, multiplied by the total length L_w of the resistive wall. Here b is the radius to the resistive wall, σ is the conductivity of the wall, and ϵ_0 is the permittivity of free space. This expression for the resistive wall wake is valid except for very small and very large z , and suffices for our purposes. For $z \rightarrow 0$, $W_{\perp}(z) \rightarrow 0$.

4. NORMAL MODES SOLUTIONS

Let us look for solutions to the equations of motion (2.18) in the form of normal modes:

$$x_i(t) = a_i e^{-i\Omega t} . \quad (4.1)$$

Here the a_i are constants, and Ω is the coherent frequency of the mode. Then, upon substituting into (2.18), the equations for the a_i 's are obtained:

$$(\Omega^2 + 2i\zeta\Omega - \omega_{\beta}^2)a_i + \sum_{j=1}^n \chi_{ij}^{\perp}(-i\Omega)a_j = 0 , \quad (4.2)$$

where we define

$$\chi_{ij}^{\perp}(s) \equiv \frac{Ne^2c}{E_0T_0} e^{-sL_{ij}/c} \sum_{q=0}^{\infty} W_{\perp}(qT_0c + L_{ij}) e^{-qT_0s} . \quad (4.3)$$

Let us substitute a transverse wake function for a resonant structure, of the form (3.1). To ensure convergence of the sums over q we may assume a small positive real

part to \bar{s} ; the solution may then be extended by analytic continuation. The result is

$$\chi_{ij}^{\perp}(s) = -\frac{Ne^2c}{E_0T_0}e^{-sL_{ij}/c} \sum_m \frac{1}{2}W_m \left[\frac{ie^{ik_mL_{ij}}}{1 - e^{(ik_m c - s)T_0}} - \frac{ie^{-ik_m^*L_{ij}}}{1 - e^{(-ik_m^* c - s)T_0}} \right] \quad (i > j) \quad ,$$

$$\chi_{ij}^{\perp}(s) = -\frac{Ne^2c}{E_0T_0}e^{-sL_{ij}/c} \sum_m \frac{1}{2}W_m \left[\frac{ie^{ik_mL_{ij}}e^{(ik_m c - s)T_0}}{1 - e^{(ik_m c - s)T_0}} - \frac{ie^{-ik_m^*L_{ij}}e^{(-ik_m^* c - s)T_0}}{1 - e^{(-ik_m^* c - s)T_0}} \right] \quad (i \leq j) \quad . \quad (4.4)$$

Alternatively, substituting the expression (3.2) for a resistive wall wake, we would obtain:

$$\chi_{ij}^{\perp}(s) = \frac{Ne^2c}{E_0T_0} \frac{2L_w}{\pi b^3} \left(\frac{c}{4\pi\epsilon_0\sigma} \right)^{1/2} e^{-sL_{ij}/c} \sum_{q=\{0, i \leq j\}}^{\infty} (qT_0c + L_{ij})^{-1/2} e^{-qT_0s} \quad . \quad (4.5)$$

Note that although the sum over q in Eq. (4.5) does not converge absolutely, it does converge for $s = -i\omega_{\beta}$, which is all that we shall need. The resistive wall contribution (4.5) should of course be added to the resonant-cavity $\chi_{ij}^{\perp}(s)$ given by (4.4), if both types of wakefield are significant.

Note that if we use the convention with $t = 0$ for all bunches at a fixed spatial reference point, so that $x_j(t - qT_0)$ is used in place of $x_j(t - qT_0 - L_{ij}/c)$ in Eq. (2.18), then the factor $e^{-sL_{ij}/c}$ does not appear in the expressions for $\chi_{ij}^{\perp}(s)$.

Eq. (4.2) involves a sum over bunches j and, via χ_{ij}^{\perp} , over turns q . The term with $i = j$ and $q = 0$ comes from the local effect of the i^{th} bunch's wake on itself. We are justified in dropping this term since the transverse wake function $W_{\perp}(z) \rightarrow 0$ as $z \rightarrow 0$; this is reflected in the above expressions for χ_{ij}^{\perp} .

If the coherent force terms are small compared to the external focusing forces, then we expect $|\Omega|$ to be close to the unperturbed betatron frequency ω_{β} . Then in

Eq. (4.2), it is convenient to approximate:

$$\Omega^2 + 2i\zeta\Omega - \omega_\beta^2 \approx 2\omega_\beta \left(\Omega - \omega_\beta + i\zeta \right) . \quad (4.6)$$

We also replace $\chi_{ij}^\perp(-i\Omega)$ by $\chi_{ij}^\perp(-i\omega_\beta)$ in Eq. (4.2). These are excellent approximations in the cases of interest to us. Then we can obtain a set of n coherent frequencies Ω , each with corresponding eigenvector \vec{a} , by solving the linear eigenvalue problem

$$\mathbf{M}\vec{a} = \Omega\vec{a} \quad , \quad (4.7)$$

where the elements of the matrix \mathbf{M} are given by

$$M_{ij} = (\omega_\beta - i\zeta)\delta_{ij} - \frac{\chi_{ij}^\perp(-i\omega_\beta)}{2\omega_\beta} \quad , \quad (4.8)$$

and \vec{a} is the vector (a_1, \dots, a_n) .

The imaginary part of the coherent frequency, $\text{Im}(\Omega)$, gives the growth rate (if positive) or damping rate (if negative) of the corresponding mode of coherent oscillation, that is to say, $1/|\text{Im}(\Omega)|$ is just the characteristic e -folding time. The components of the corresponding eigenvector are of course complex, and give the relative phase and amplitude of each bunch in that oscillation mode.

5. DAMPING MECHANISMS

The purpose of a damping ring is to reduce the transverse emittance of the bunches of electrons or positrons circulating in it. This occurs as each particle in a bunch emits synchrotron photons essentially along its direction of motion (which has a small transverse betatron component), and then regains the lost energy via purely longitudinal acceleration by the rf system. This is an incoherent process — each particle gains and loses energy independently of what the other particles are doing.

It can be shown under quite general assumptions that the longitudinal and transverse oscillations of an individual particle in a bunch are exponentially damped by synchrotron radiation,¹³ with damping time constants given by

$$\tau_i = \frac{2E_0 T_0}{J_i U_0} \quad , \quad (5.1)$$

and where the damping partition numbers J_i satisfy¹⁴

$$J_x + J_y + J_\epsilon = 4 \quad . \quad (5.2)$$

Here U_0 is the radiation loss per orbital period T_0 , and E_0 is the energy, for a particle on the design orbit. In the damping ring designs that we shall consider, the damping times are a few milliseconds. Radiation damping does not result in arbitrarily small emittances in either the longitudinal or transverse direction, since the radiation is emitted as discrete photons. Ultimately, the equilibrium emittance is determined by the interaction between the radiation damping and the “quantum excitation” due to the discrete nature of the photon emission.

However, the bunches cannot be injected exactly onto the equilibrium orbit, and thus each bunch also starts out with a small *coherent* betatron oscillation. It is of

course this coherent bunch motion that we are really concerned with here, and which we have approximated as the dipole oscillations of a rigid bunch. The transverse offset of a bunch induces a transverse wakefield, which can further excite the coherent betatron motion of trailing bunches. However, there are some additional damping mechanisms that can play an important role in counteracting this wakefield excitation.

One such mechanism is “Landau damping”, which occurs when there is a spread in the oscillation frequencies of different particles in a bunch. Thus, even if a bunch starts out with a coherent oscillation as shown in Figure 1(a), after awhile the individual oscillations lose coherence. If the particles have spread out in phase space as shown in Figure 1(b), there is no longer any coherent oscillation, but the effective emittance is blown up. However, synchrotron radiation eventually reduces the emittance as shown in Figure 1(c). Obviously, this particular figure is drawn assuming that the decoherence time scale is much faster than the synchrotron damping time scale. Also, note that the size of the coherent offset has been exaggerated in the figure for clarity; in reality it would be closer to the bunch size.

The usual criterion for Landau damping to be effective at stopping an instability with coherent frequency Ω is¹⁵

$$|\Omega - \omega| < \Delta\omega \quad , \quad (5.3)$$

where ω is the unperturbed oscillation frequency (betatron in the present case), and $\Delta\omega$ is the incoherent frequency spread within the bunch. In other words, the spread in frequencies $\Delta\omega$ gives a threshold for the coherent frequency shifts, below which Landau damping can be expected to wash out the exponential growth of an unstable coherent oscillation.

One source of such an incoherent frequency spread, and thus Landau damping, is

the amplitude dependence of the betatron tune of individual particles in the bunch. This is most significant right after injection, when it could be quite large.

There is also a tune spread due to space charge.¹⁶ For a bunched beam, this tune spread may be written

$$\Delta\nu = \frac{1}{(2\pi)^{3/2}} \frac{\bar{\beta} r_e N c T_0}{\gamma^3 \sigma_z a^2} F \quad (5.4)$$

Here $r_e \equiv e^2/mc^2 \approx 2.82 \times 10^{-15} \text{m}$, $\bar{\beta}$ is the average horizontal or vertical beta function in the ring, and σ_z is the bunch length. For a round bunch, a is the bunch radius and the form factor F is equal to 1. For a flat bunch ($R \gg 1$, where R is the ratio of the bunch width to the bunch height), we take a to be the horizontal bunch width, in which case $F \sim 2$ horizontally and $F \sim 2R$ vertically.¹⁷ Other symbols are as previously defined. In the damping ring design example to be considered here, the bunch starts out round and ends up with a final aspect ratio $R \sim 10$. The tune spread given by Eq. (5.4) may be significant at or soon after injection. For $a \sim 100 \mu\text{m}$ and $F \sim 1$, taking other parameters from those in Table 1, we obtain $\Delta\nu \sim 0.0006$. With this value of tune spread, the bunch would decohere completely as in Fig. 1(b), after about 2000 turns. This is only a small fraction of the more than 50000 turns that a bunch spends in the ring.

Thus, one possibility is that there is strong Landau damping of the coherent betatron oscillation soon after injection, if the tune spread is large enough. However, there is another mechanism which may both preserve the coherence of the bunch yet damp the coherent oscillation. This is the head-tail effect,¹⁸ which is a result of the circulation of particles between the head and tail of the bunch as they undergo synchrotron oscillations. The damping (or anti-damping) rate is proportional to the

magnitude of the chromaticity ξ , defined by

$$\delta\nu \equiv \xi \frac{\Delta p}{p_0} = \xi \frac{\Delta E}{E_0} \quad (5.5)$$

Here $\delta\nu$ is the change in tune due to the deviation Δp from the design-orbit momentum p_0 ; the last equality follows from the assumption that the particles are highly relativistic. For positive chromaticity there is damping, and for negative chromaticity there is anti-damping; for this and other reasons, the focusing lattice will be designed to give positive chromaticity. The damping rate can be calculated from the short range wakefield, given the impedance of the vacuum chamber.¹⁸⁻²⁰ For our damping ring design example, and using a simple broad-band impedance model, one obtains a coherent head tail damping rate more than ten times faster than the synchrotron damping rates, for a typical (~ 1) value of the chromaticity.

The two regimes of 1) large tune spread with rapid decoherence via Landau damping, and 2) coherent head-tail damping, have been observed experimentally in existing storage rings.²¹ Which mechanisms dominate in future damping rings will depend on their detailed design. Here we shall use the coherent head-tail damping as an estimate of the damping parameter ζ that one might expect. Note that the coherent head tail damping is exponential. Landau damping, if important, may lead to much faster (and non-exponential) damping of an injected coherent betatron oscillation.

6. LAPLACE TRANSFORM SOLUTION

We turn now to the discussion of the methods for obtaining the motion of the bunches as a function of time (or number of turns through the ring). This enables us to study the transient behavior, which is of particular interest in damping rings. In this section we discuss the first such method, namely the use of the Laplace transform.

Defining

$$\tilde{x}_i(s) \equiv \int_0^{\infty} e^{-st} x_i(t) dt \quad , \quad (6.1)$$

performing the Laplace transform on Eq. (2.18), and rearranging terms we obtain

$$\sum_{j=1}^n \left[(s^2 + 2\zeta s + \omega_\beta^2) \delta_{ij} - \chi_{ij}^\perp(s) \right] \tilde{x}_j(s) = (s + 2\zeta) x_i(0) + \dot{x}_i(0) \quad . \quad (6.2)$$

Let us define $A_{ij}(s)$ to be the quantity in square brackets divided by $2\omega_\beta$. The roots of $\det \mathbf{A} = 0$ are easily seen to be $s = i\Omega_k$, where the Ω_k 's are the coherent frequencies obtained in the normal modes analysis. Here we assume, consistent with that analysis, that the roots $-i\Omega_k$ are near $-i\omega_\beta$, so that

$$2\omega_\beta A_{ij} \approx [-2i\omega_\beta(s + i\omega_\beta) - 2i\omega_\beta\zeta] \delta_{ij} - \chi_{ij}^\perp(-i\omega_\beta) \quad , \quad (6.3)$$

from which, as one would expect, we get

$$A_{ij}(-i\Omega) = M_{ij} - \Omega \delta_{ij} \quad . \quad (6.4)$$

Solving Eq. (6.2) to obtain the \tilde{x}_i yields

$$\tilde{x}_i(s) = \frac{1}{2\omega_\beta} \sum_{j=1}^n \frac{c_{ji}}{\det \mathbf{A}} [(s + 2\zeta) x_j(0) + \dot{x}_j(0)] \quad . \quad (6.5)$$

Here $c_{ji}(s)$ is the j^{th} cofactor of the matrix \mathbf{A} , that is, for $\det \mathbf{A} \neq 0$,

$$(c_{ji}/\det \mathbf{A}) = (\mathbf{A}^{-1})_{ij} \quad . \quad (6.6)$$

Taking the inverse Laplace transform we obtain

$$x_i(t) = \frac{1}{2\pi i} \int_C e^{st} \sum_{j=1}^n \frac{c_{ji}(s)[(s+2\zeta)x_j(0) + \dot{x}_j(0)]}{2\omega_\beta(-i)^n \prod_{k=1}^n (s+i\Omega_k)} \quad , \quad (6.7)$$

where the contour C is parallel to the imaginary axis and to the right of all the poles. Closing the contour to the left and applying the residue theorem, we obtain the solutions for the offsets as a function of time:

$$x_i(t) = \sum_{l=1}^n \frac{\sum_{j=1}^n c_{ji}(-i\Omega_l)[(-i\Omega_l+2\zeta)x_j(0) + \dot{x}_j(0)]}{(-2i\omega_\beta) \prod_{\substack{k=1 \\ k \neq l}}^n (-\Omega_l + \Omega_k)} e^{-i\Omega_l t} \quad . \quad (6.8)$$

This can be evaluated numerically once we have obtained the coherent frequencies Ω_l as discussed earlier. This solution is valid provided that all n of the coherent frequencies are different from each other, as is normally the case. If all the wakefields were very strongly damped, then some of the Ω_i 's could become nearly degenerate. In this event, there will be problems attempting to solve Eq. (6.8) numerically. In practice, even if the cavity wakes are strongly damped, the resistive wall wake is strong enough to prevent this degeneracy. Obviously, if there is a true degeneracy in the problem, then Eq. (6.8) must be modified appropriately.

7. TRACKING

An alternate method of obtaining the individual bunch offsets as a function of turn number is to use tracking. This method is useful when studying rings in which the cavity transverse wakefield is strongly damped.

In our tracking simulation, the force due to the wakefield is represented by a localized kick at one point in the ring. As was shown in Appendix A, this is justified even if the wake force is actually distributed around the ring, provided that the coherent tune shift due to the wake is much less than $\frac{1}{2\pi}$. Then the wakes due to rf cavities at more than one location and/or the resistive wall wake can be lumped together into a kick at a single point.

We look at the offset and slope of each bunch at the rf cavity. The motion of a bunch on a given turn is divided into two parts, the first part being a mapping around the ring, in accordance with Eq. (2.8), from just after the kick point all the way around the ring to where the bunch is about to get kicked again (for simplicity we assume $\beta' = 0$ at the kick point):

$$\begin{pmatrix} x_i \\ x'_i \end{pmatrix} \longrightarrow e^{-\zeta T_0} \begin{pmatrix} \cos \mu & \beta \sin \mu \\ -\frac{1}{\beta} \sin \mu & \cos \mu \end{pmatrix} \begin{pmatrix} x_i \\ x'_i \end{pmatrix} . \quad (7.1)$$

Primes denote derivatives with respect to longitudinal distance, and μ is the coherent betatron phase advance around the ring. Recall that T_0 is the orbital period, and ζ is the coherent damping parameter.

The present turn through the ring is completed by the localized kick:

$$x_i \longrightarrow x_i$$

$$x'_i \longrightarrow x'_i + \frac{Ne^2}{E_0} \sum_{q=0}^{q_{max}} \sum_{j=1}^n W_{\perp}(L_{ij} + qC) x_{j,q} , \quad (7.2)$$

Passing through the kick point changes the slope, but not the offset of the bunch.

Here $x_{j,q}^-$ denotes the offset at the kick point of the j^{th} bunch q turns ago (note that $q = 0$ is just the present turn).

The value of q_{max} must be large enough that the wakefields are negligible after q_{max} turns; therefore this method is less practical than the Laplace transform method when there are many bunches and very long-range wakes.

8. COMPARISON OF LAPLACE TRANSFORM AND TRACKING METHODS

For $n = 100$ bunches, the tracking method is slow, especially if one needs to keep track of wakefield effects persisting for more than a turn. Generally we do want to keep track of wakes from preceding turns, since even if we strongly damp all the transverse modes in the rf cavities, there is still a resistive wall wake that only falls off as $z^{-1/2}$.

However, the computation of the coherent frequencies and eigenmodes by the formalism presented here takes relatively little time for 100 bunches. The results of this computation may then be used to compute the offset of any of the bunches as a function of turns through the ring, using a program implementing the Laplace transform method discussed earlier. The plots of bunch offset versus turns obtained using the Laplace transform method are indistinguishable from those obtained using the tracking method.

For some purposes, a knowledge of the maximum growth rates to be expected is all that is needed. However it is possible to have transient blow-up due to interference, even when the imaginary parts of all coherent frequencies are negative (illustrations of this behavior will be seen later in some of the examples). In designing a damping ring, it is essential to have a large enough aperture to accommodate such transients,

or, better still, reduce the wakefields (and/or increase the coherent damping) so that transient blow-up is eliminated.

Note that there is also another type of transient behavior due to the fact that trains are being injected or extracted one at a time, while the other trains in the ring are at various intermediate stages of damping. Although the cavity wakefields may be strongly damped, there can still be a small but significant coupling between trains due to the resistive wall wakefield. This means that the effect on a train due to the injection and extraction of other trains must be taken into account. Using either the tracking method or the Laplace transform method, one may study the details of this behavior.

9. DAMPING RING PARAMETERS

In the remainder of this paper, we give examples of the application of our methods to the study of a damping ring design with ten trains of ten bunches each. Parameters for a such a damping ring, suitable for a next-generation linear collider^{22,23} are given in Table 1. This design utilizes wigglers to reduce the damping times.

9.1. THE RF SYSTEM

We shall use two examples of rf cavity design. First we shall consider a typical cavity with nose cones, namely the PEP cavity scaled to the desired rf frequency of about 1.4 GHz. We shall assume that the parasitic modes are damped by conventional means to Q values of about 500. In the following discussions, we shall refer to this cavity design as the “conventional cavity”.

Next we shall consider a newer type of cavity design, that strongly damps the parasitic modes by means of slots coupled to radial waveguides.^{24–26} Our particular

example is a pillbox cavity with a relatively large ratio of iris radius to rf wavelength ($a/\lambda_{rf} \approx 0.2$); the cavity is assumed to have very low Q 's (see below) obtained by means of such damping slots. We shall refer to this design as the "damped cavity".

More detailed information on the modes for each cavity is given in Appendix B.

The voltage \hat{V}_g specified for the rf system is 0.75 MeV (Refs. 22 and 23). The number N_{cells} of rf cells required is given by

$$\hat{V} = N_{cells} L_{cell} \hat{\mathcal{E}}_z \quad , \quad (9.1)$$

where \hat{V} is the peak cavity voltage, L_{cell} is the length of a cell and $\hat{\mathcal{E}}_z$ is the average accelerating field experienced by a relativistic particle as it traverses the structure (on the crest of the rf wave). For normal rf, $\hat{\mathcal{E}}_z$ should not be more than about 1 MeV/m, in which case the required number of rf cells is $N_{cells} \approx 10$. This is the number of cells we shall assume in our examples; however, note that if it were necessary to have more voltage or fewer cells, one could use a superconducting rf system (or normal rf with superconducting cavity shape), which could sustain a much higher gradient. This could considerably reduce the required number of cells and hence the transverse wakefield of the rf system.

Note that the coupled-bunch growth rates due to the rf system can be scaled by multiplying those for a single cell by the total number of cells, so long as we are assuming strongly damped transverse wake modes. Cavity-to-cavity frequency spreads, which would effectively broaden the cavity resonances for high- Q modes, are irrelevant here since the higher-order resonances are already broadened due to the strong damping.

9.2. SMOOTH FOCUSING FUNCTION

For our purposes, we represent the focusing lattice by a constant average beta function. Taking the value of betatron tune for the y -direction, $\nu_y = 11.27$, and ring circumference $C = 155.1$ m from Table 1, we obtain $\bar{\beta} = 2.2$ m, which is the value that we shall use in our examples. The average focusing is about twice as strong in the x -direction.

9.3. EMITTANCE AND INJECTION REQUIREMENTS

The normalized emittance $\gamma\epsilon_i$ of the injected positron beam is about 3 mm rad in both the x and y directions, and the normalized emittance of the injected electron beam is about an order of magnitude smaller. The required normalized emittances upon extraction from the damping rings are $\gamma\epsilon_x = 3.0$ $\mu\text{m rad}$ and $\gamma\epsilon_y = 30$ nm rad. The damping rings are designed to be able to handle the worst case, namely the positrons.

The transverse rms sizes $\sigma_x = \sqrt{\epsilon_x\beta_x}$ and $\sigma_y = \sqrt{\epsilon_y\beta_y}$ of an injected positron bunch are thus about 0.6 mm (taking the beta function to be 2.2 m). To avoid significantly diluting the positron emittance via initial decoherence of the beam particles, the beams must be injected to within less than a positron beam size of the axis; it is expected that they can easily be injected to within less than 0.1 mm. Given that the electrons are injected to within a similar absolute tolerance, they will also have sufficient time to damp even if they should suffer some dilution, since their emittance is much smaller to begin with.

Assuming the above design emittances, the transverse rms dimensions at extraction are $\sigma_x \approx 40$ μm and $\sigma_y \approx 4$ μm . The amplitude of the coherent betatron

oscillation of a bunch is

$$\hat{x} = [x^2 + (\beta x')^2]^{1/2} = [x^2 + (\dot{x}/\omega_\beta)^2]^{1/2} . \quad (9.2)$$

This amplitude at the time of extraction from the damping ring needs to be much smaller than the vertical bunch size $\sigma_y \approx 4 \mu\text{m}$, to avoid position jitter downstream.

9.4. INITIAL CONDITIONS

We assume that the bunches in a train each have the same offset, x_0 , at the time when the train is injected into the damping ring. As already noted, only one train at a time is to be injected or extracted from a damping ring containing multiple bunch trains, so each bunch train will be at a different stage of damping, depending on how long it has been in the ring. For simplicity in the simulation, all the bunches in all trains are started out with the offset x_0 , and enough injection and extraction cycles are performed so that transients from this artificial initial condition have died away. It is assumed that a given train is extracted and replaced with a new train of offset x_0 ; the order of replacement of trains is assumed to be in the direction of motion of the bunches, so that a train that is about to be extracted is not disturbed by injecting a new train of offset x_0 (and thus larger wakefields) right in front of it.

Since the equations of motion are linear, we do not yet specify the actual size of the offset; the simulation results may be expressed in terms of x/x_0 .

9.5. THE VACUUM CHAMBER

For our calculations, we shall assume the vacuum chamber outside the rf cavities to be a smooth metal pipe of constant radius b . The larger b is, the weaker the wakefields will be; note from Eq. (3.2) that the dependence of the transverse wakefield

on b is quite pronounced ($\sim b^{-3}$). However, smaller b is less expensive, and we would like to keep the radius b to about a centimeter.

The resistive wall wakefield also scales as $\sigma^{-1/2}$, where σ is the conductivity of the wall. The conductivities of materials one might consider using for the wall are: copper, about 5.9×10^7 mho/m, aluminum slightly less (2.5×10^7 mho/m), and stainless steel more than an order of magnitude less (1.4×10^6 mho/m).

We have calculated the coherent frequencies of the 100 modes of transverse oscillation of 100 bunches, using the parameters in Table 1 and assuming only a resistive wall wakefield. Using the conductivity of copper and radius 1 cm, the largest growth rate among the 100 modes is about 430 sec^{-1} . We can scale with conductivity and wall radius to obtain the characteristic growth times due to any resistive wall of the same length. Thus we obtain

$$\tau \approx (2.3 \text{ msec}) \left(\frac{\sigma}{\sigma_{Cu}} \right)^{1/2} \left(\frac{b}{1 \text{ cm}} \right)^3 . \quad (9.3)$$

We see that the contribution of the transverse resistive wall wake can be significant, even for the relatively favorable case of copper.

10. RESULTS FOR CONVENTIONAL CAVITY

In this section we discuss results on the transverse coupled-bunch instability, assuming an rf system utilizing the conventional cavity design with $Q = 500$. Ring parameters are as given in Table 1. We begin by considering a single train of ten bunches injected into the ring. For comparison, we first show in Fig. 2 plots of the transverse offset vs. turn number, for the first and last bunch in the train, with no resistive wall wake included. The coherent damping assumed is $\zeta = 900 \text{ sec}^{-1}$, i.e., a characteristic coherent damping time $1/\zeta \approx 1 \text{ msec}$. We see that there is a

transient blow-up of about a factor of four, in the last bunch in the train, even though it is long-term stable (the imaginary part of each of the ten coherent frequencies is negative).

In Fig. 3, we include the resistive wall wake due to a copper vacuum pipe with a 1 cm radius; other than this, all parameters are the same as in Fig. 2. The transient blow-up of the last bunch has increased to about 6.5, and there is some noticeable blow-up of the first bunch in the train since it is now feeling the transverse resistive wall wake left by previous passages of the bunch train.

If we try to put ten such bunch trains into the ring, then even the long term stability is lost — all the bunches have blown up completely before 10000 turns. The coherent damping parameter is expected to be larger than the value we have used in this example, but it would still be wise to reduce the size of the wakefields in order to strongly attenuate the coupling between bunch trains. Although we will still have the long-range resistive wall wake to contend with, we can virtually eliminate the cavity contribution to the long-range wake by using damped cavities. Thus we turn to the use of this cavity design in our remaining examples.

11. RESULTS FOR MODE-DAMPED CAVITY

For the examples in this section, we shall assume an rf system consisting of damped acceleration cavities (Refs. 24, 25, and 26). Calculation of the Q 's of the transverse modes in such cavities shows that they can be very low. We shall take a conservative value $Q = 30$ for all these modes, although at least some of them may be significantly lower.²⁷ Ten resonant cavity dipole modes were included, of which the first (lowest frequency) is strongly dominant because of the large iris. The transverse growth and damping rates will be sensitive to the frequency of this dominant mode.

Even though its frequency could be tuned to a more favorable value, we choose the somewhat pessimistic situation in which the wakefield is near a peak of its oscillation at one bunch spacing. With $Q = 30$, there is about 0.13 e -folding of the fundamental transverse mode between adjacent bunches within a train, and nearly 10 e -foldings between bunch trains (and more e -foldings for the higher-order modes). There is still, however, the resistive wall wake producing some coupling between bunch trains.

At a repetition rate of 360 Hz, there are 5369 turns between successive injections and extractions. Thus each of the ten trains spends a total of 53690 turns in the ring. For computational convenience, the bunches are all started out with the same offset x_0 , and we shall show the results beginning after all bunch trains have been extracted and replaced at least once.

In our first example using this cavity we use the same coherent damping as was used in the conventional cavity examples just discussed, namely $\zeta = 900 \text{ sec}^{-1}$. Thus the characteristic damping time in this example, $1/\zeta = 1 \text{ msec}$, is roughly four times faster than the synchrotron radiation damping times (see Table 1). Fig. 4(a) shows the first bunch and Fig. 4(b) the last bunch in a train, where there are a total of ten such trains. Fig. 4(c) and Fig. 4(d) are the same as Fig. 4(a) and Fig. 4(b) respectively, except for an expanded vertical scale to show the size of the offsets after damping. In Fig. 5, the coherent damping has been increased to about ten times the synchrotron radiation damping rate, that is, $\zeta = 2500 \text{ sec}^{-1}$.

In both of these cases, there is long-term stability, however we must examine whether the coherent betatron oscillation at extraction is small enough compared to the extracted beam size. For $\zeta = 900 \text{ sec}^{-1}$, the coherent betatron oscillation amplitude calculated from Eq. (9.2) is approximately 2×10^{-2} (dimensionless) at extraction, for the bunch in the train which has the largest offset; that is, the ratio of

the final coherent oscillation amplitude to the initial offset is about 2×10^{-2} . Assuming that the initial offset is about 0.1 mm, the final coherent oscillation amplitude of the extracted bunches may be as large as $2 \mu\text{m}$. This is comparable to the vertical beam size σ_y and thus too large to be acceptable.

For $\zeta = 2500 \text{ sec}^{-1}$, the largest coherent betatron oscillation amplitude at extraction is about $0.02 \mu\text{m}$, again assuming an initial amplitude of 0.1 mm. This gives an acceptable result since it is much less than the vertical extracted beam size $\sigma_y = 2 \mu\text{m}$. As noted earlier, the contribution of coherent head-tail damping to the value of ζ was calculated to be at least as large as the value used in this example.

12. CONCLUSIONS

We have presented a formalism for calculating the growth and damping rates of the normal modes of transverse coupled-bunch oscillation, suitable for a very general form of the transverse dipole wakefield and arbitrary placement of the bunches. Two methods of obtaining the "time-domain" behavior (transverse offsets of the bunches versus turns in the ring) were also given, one utilizing the results of the normal modes formalism and one a simple (but in some cases, much more computationally expensive) tracking. Examples of applications to the study of the damping rings of future linear colliders were discussed. It is found that with the expected amount of coherent damping and with an rf system based on mode-damped cavities, the instability is adequately controlled.

13. ACKNOWLEDGMENTS

We would like to thank Z.D. Farkas, K. Kubo, P. Morton, T. Raubenheimer, J. Urakawa, and P. Wilson for useful discussions related to this work.

This work was supported by Department of Energy contract DE-AC03-76SF00515.

APPENDIX A

We wish to show that the coherent tune shift $\delta\nu$ due to the wakefield is the same whether we represent the wake by a localized kick or by an equivalent distributed force, provided that $2\pi\delta\nu \ll 1$.

We write the tune as $\nu = \nu_0 + \delta\nu$, where ν_0 is the tune due to the lattice beta function. As in the main body of the paper, we replace the alternating gradient focusing lattice by an average beta function β that is a constant all around the ring, so that $\nu_0 = C/(2\pi\beta)$, where C is the ring circumference. First, note that $\delta\nu$ would not be small if the ring were running near an integer or half-integer resonance, i.e., if $\sin 2\pi\nu_0$ is near zero; clearly we must assume the ring is away from such resonances.

For simplicity, we consider the case of a single bunch, for the two extremes of a delta function wake and the equivalent constant wake distributed over the entire ring circumference. The equation of motion for the transverse offset x , for the case of the distributed wake, is of the form:

$$x'' + \frac{1}{\beta^2}x + a_1x = 0 \quad , \quad (\text{A.1})$$

where a_1 is a constant representing the effective force due to the wake. The equivalent equation of motion for a delta-function kick is

$$x'' + \frac{1}{\beta^2}x + a_2\delta(s)x = 0 \quad , \quad (\text{A.2})$$

where $a_2 = a_1C$.

The tune ν for the distributed wake case is given by

$$2\pi\nu = \left(\frac{1}{\beta^2} + a_1 \right)^{1/2} C \quad . \quad (\text{A.3})$$

Using $\bar{C} = 2\pi\nu_0\beta$, this becomes

$$\nu = \nu_0 + \delta\nu = \nu_0(1 + \beta^2 a_1)^{1/2} . \quad (\text{A.4})$$

Provided that $\delta\nu \ll \nu_0$, we can expand the square root to obtain

$$\delta\nu \approx \frac{\nu_0\beta^2 a_1}{2} = \frac{\beta C a_1}{4\pi} = \frac{\beta a_2}{4\pi} . \quad (\text{A.5})$$

The tune for the delta-function wake case (A.2) is related to the trace of the corresponding transfer matrix as follows:

$$\cos(2\pi\nu) = \frac{1}{2} \text{Tr} \left[\begin{pmatrix} \cos(2\pi\nu_0) & \beta \sin(2\pi\nu_0) \\ -\frac{1}{\beta} \sin(2\pi\nu_0) & \cos(2\pi\nu_0) \end{pmatrix} \begin{pmatrix} 1 & 0 \\ -a_2 & 1 \end{pmatrix} \right] . \quad (\text{A.6})$$

This yields

$$\cos(2\pi\nu_0) \cos(2\pi\delta\nu) - \sin(2\pi\nu_0) \sin(2\pi\delta\nu) = \cos(2\pi\nu_0) - \frac{a_2\beta}{2} \sin(2\pi\nu_0) . \quad (\text{A.7})$$

For $2\pi\delta\nu \ll 1$, this becomes

$$\delta\nu \approx \frac{\beta a_2}{4\pi} , \quad (\text{A.8})$$

which is the same as the distributed wake case (A.5).

Typically ν_0 is considerably larger than $\frac{1}{2\pi}$, so the more stringent of the assumptions made is that $\delta\nu \ll \frac{1}{2\pi}$ (as noted already, a necessary condition is that the ring be sufficiently far from resonances). Given that this holds, we have shown that it doesn't matter whether the wake force is lumped or distributed; the resulting tune shift is the same in either case.

APPENDIX B

The coefficients W_m in Eq. (3.1) may be expressed in terms of the transverse loss factors κ_m , the spatial frequencies k_m , and the iris radius a , as follows (see Ref. 8):

$$W_m = \frac{2\kappa_m}{a^2 k_m} \quad . \quad (B.1)$$

where the transverse loss factors are evaluated at the iris radius. For the conventional cavity, $a = 1.25$ cm, and for the damped cavity $a = 4.16$ cm.

The loss factor has units [V/C], and is related to the transverse shunt impedance R of the mode by

$$\kappa = \frac{\omega}{4} \left(\frac{R}{Q} \right) \quad . \quad (B.2)$$

(Caution: If the “circuit definition” rather than the “accelerator definition” is used for the shunt impedance R , then the factor 1/4 on the right hand side of Eq. (B.2) becomes 1/2.)

The frequencies and loss factors for the transverse dipole modes of these cavities are shown in Table 2 for the conventional cavity, and in Table 3 for the damped cavity. As noted previously, the Q 's of the conventional cavity are all assumed to be damped by conventional means to a value of 500, while the Q 's of the damped cavity are assumed to be 30, although they could in reality be much lower.

In both cases, there are assumed to be a total of 10 rf cells.

REFERENCES

1. See for example *High Energy Physics in the 1990's*, proceedings, Snowmass, Colorado, 1988, edited by S. Jensen (World Scientific, Teaneck, NJ, 1988); or *Linear Collider Working Group Reports from Snowmass '88*, edited by R.D. Ruth (Report No. SLAC-334, Stanford, 1989).
2. K.A. Thompson and R.D. Ruth, *Phys.Rev.D*, **41**, 964 (1990).
3. E.D. Courant and A.M. Sessler, *Rev. Sci. Instr.*, **37**, 1579 (1966).
4. B. Zotter and F. Sacherer, in *Proceedings of the First Course of the International School of Particle Accelerators of the 'Ettore Majorana' Centre for Scientific Culture*, Erice, Italy, 1976, edited by M.H. Blewett (CERN 77-13).
5. A.W. Chao, in *Physics of High Energy Particle Accelerators*, [Stanford Linear Accelerator Center, Stanford, California], edited by M. Month (AIP Conf. Proc. No. 105) (AIP, New York, 1982).
6. K.A. Thompson, in *Proceedings of the Tau-Charm Factory Workshop*, [Stanford Linear Accelerator Center, Stanford, California], edited by L.V. Beers, Report No. SLAC-343 (1989).
7. E.D. Courant and H.S. Snyder, *Annals of Physics*, **3**, 1 (1958).
8. K.Bane, in *Physics of Particle Accelerators*, edited by M. Month and M. Dienes (AIP Conf. Proc. No. 153) (AIP, New York, 1987).
9. See also Ref. 5 for a general discussion of wake functions.
10. T. Weiland, *Nucl. Instr. Meth.* **216**, 329 (1983).
11. K. Bane and B. Zotter, in *11th International Conference on High Energy Accelerators*, Geneva, Switzerland, 1980, edited by W.S. Newman (Experimentia, Supplementum Vol. 40) (Birkhäuser, Basel, 1980).

12. L.J. Laslett, V.K. Neil, and A.M. Sessler, *Rev. Sci. Instr.* **36**, 436 (1965);
P.L. Morton, V.K. Neil, and A.M. Sessler, *J. Appl. Phys.*, **37**, 3875 (1966); see
also Ref. 5.
13. M. Sands, Report No. SLAC-121 (1970).
14. K. Robinson, *Phys. Rev.*, **111**, 373 (1958).
15. L.J. Laslett, V.K. Neil, and A.M. Sessler, *Rev. Sci. Instr.* **36**, 426 (1965).
16. L.J. Laslett, Report No. BNL-7534 (1963).
17. T. Raubenheimer, private communication.
18. C. Pellegrini, *Nuovo Cimento* **64A**, Series 10, 447 (1969).
19. R.D. Ruth, Report No. BNL-51425 (1981).
20. R.D. Ruth, in *12th International Conference on High Energy Accelerators*,
Fermi National Accelerator Laboratory, Batavia, Illinois, 1983.
21. The SPEAR Group, in *Proceedings of the Ninth International Conference
on High Energy Accelerators*, Stanford Linear Accelerator Center, Stanford,
California, 1974.
22. T. Raubenheimer, L.Z. Rivkin, and R.D. Ruth, in *High Energy Physics in the
1990's*, proceedings, Snowmass, Colorado, 1988, edited by S. Jensen (World
Scientific, Teaneck, NJ, 1988); in *Linear Collider Working Group Reports from
Snowmass '88*, edited by R.D. Ruth (Report No. SLAC-334, Stanford, 1989).
23. T.O. Raubenheimer, W.E. Gabella, P.L. Morton, M.J. Lee, L.Z. Rivkin, and
R.D. Ruth, *I.E.E.E. Particle Accelerator Conference Proceedings* (1989), Re-
port No. SLAC-PUB-4912.
24. R.B. Palmer, in *High Energy Physics in the 1990's*, proceedings, Snowmass,
Colorado, 1988, edited by S. Jensen (World Scientific, Teaneck, NJ, 1988);
Report No. SLAC-PUB-4542 (unpublished); in *Linear Collider Working Group*

Reports from Snowmass '88, edited by R.D. Ruth (Report No. SLAC-334, Stanford,1989).

25. H. Deruyter, et.al., I.E.E.E. Particle Accelerator Conference Proceedings (1989), Report No. SLAC-PUB-4865.
26. H. Deruyter, et.al., presented at 2nd European Particle Accelerator Conference, June 12-16,1990, Report No. SLAC-PUB-5263.
27. N.M. Kroll and D.U.L.Yu, submitted to Part. Accel.; Report No. SLAC-PUB-5171 (January, 1990).

TABLE CAPTIONS

- 1: Damping ring parameters for examples given in text.
- 2: Frequencies and loss factors of the the transverse dipole modes for the conventional cavity.
- 3: Frequencies and loss factors of the the transverse dipole modes for the damped cavity.

Number of bunch trains	10
Number of bunches per train	10
Number of particles per bunch, N	2×10^{10}
Particle energy, E_0	1.8 GeV
Damping ring circumference	155.1 m
rf frequency	1.428 GHz
Bunch spacing within a train	$1 \lambda_{rf} \approx 21.0$ cm
Horizontal betatron tune	24.37
Vertical betatron tune	11.27
Momentum compaction factor, α	1.2×10^{-3}
Peak rf generator voltage, \hat{V}_g	0.75 MeV
Horizontal synchrotron damping time, τ_x	2.50 msec
Vertical synchrotron damping time, τ_y	3.98 msec
Longitudinal synchrotron damping time, τ_ϵ	2.82 msec
Synchrotron radiation loss per turn, U_0	468 KeV
Bunch length, σ_z	4.6 mm
Fractional energy spread, σ_ϵ	0.00104
Repetition rate	360 Hz

Frequency f (GHz)	Loss factor κ (V/pC)
2.022669	0.0056
2.533394	0.0076
3.095458	0.1408
3.401970	0.0040
3.866890	0.0144
4.185043	0.0120
4.361010	0.0720
4.373034	0.2328
4.884713	0.0144
4.968498	0.0428
5.464145	0.2440
5.568161	0.0012
5.847952	0.0016
6.411544	0.0052
6.419560	0.0920
6.563463	0.0052
6.783327	0.2000

Frequency f (GHz)	Loss factor κ (V/pC)
1.836724	0.289957
3.041532	0.046032
3.616563	0.020256
3.789505	0.015430
4.464128	0.029499
4.783138	0.035627
5.339451	0.011505
5.581285	0.038116
5.831103	0.013636
6.450126	0.037458

FIGURE CAPTIONS

- 1) Phase space of a bunch (a) upon injection with a coherent oscillation, (b) after decoherence due to a tune spread, (c) after synchrotron radiation has damped the incoherent oscillations.
- 2) Transverse bunch offset (divided by the initial offset x_0 of the bunches) vs turn number for (a) the first bunch, and (b) the last bunch in a single train of ten bunches, assuming the conventional cavity design and no resistive wall wake. The coherent damping assumed is $\zeta = 900 \text{ sec}^{-1}$.
- 3) Transverse bunch offset (divided by x_0) vs turn number for (a) the first bunch, and (b) the last bunch in a single train of ten bunches, assuming the conventional cavity design and a resistive wall wake. The coherent damping assumed is $\zeta = 900 \text{ sec}^{-1}$.
- 4) Transverse bunch offset (divided by x_0) vs turn number for (a) the first bunch, and (b) the last bunch, in the last of ten trains of ten bunches, including the mode-damped-cavity and resistive wall wakes. The coherent damping assumed is $\zeta = 900 \text{ sec}^{-1}$. Parts (c) and (d) are the same as parts (a) and (b) respectively, except for an expanded vertical scale.
- 5) Transverse bunch offset (divided by x_0) vs turn number for (a) the first bunch, and (b) the last bunch, in the last of ten trains of ten bunches, including the mode-damped-cavity and resistive wall wakes. the coherent damping assumed is $\zeta = 2500 \text{ sec}^{-1}$. Parts (c) and (d) are the same as parts (a) and (b) respectively, except for an expanded vertical scale.

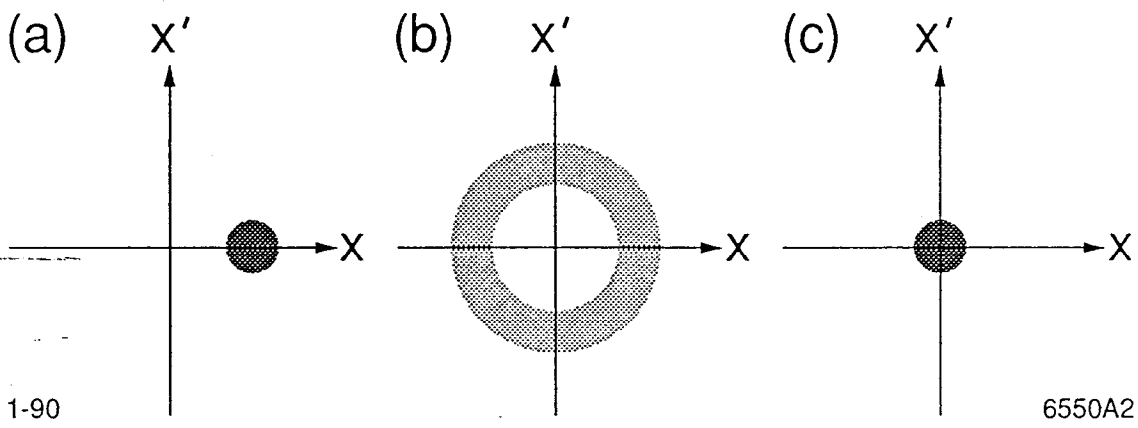
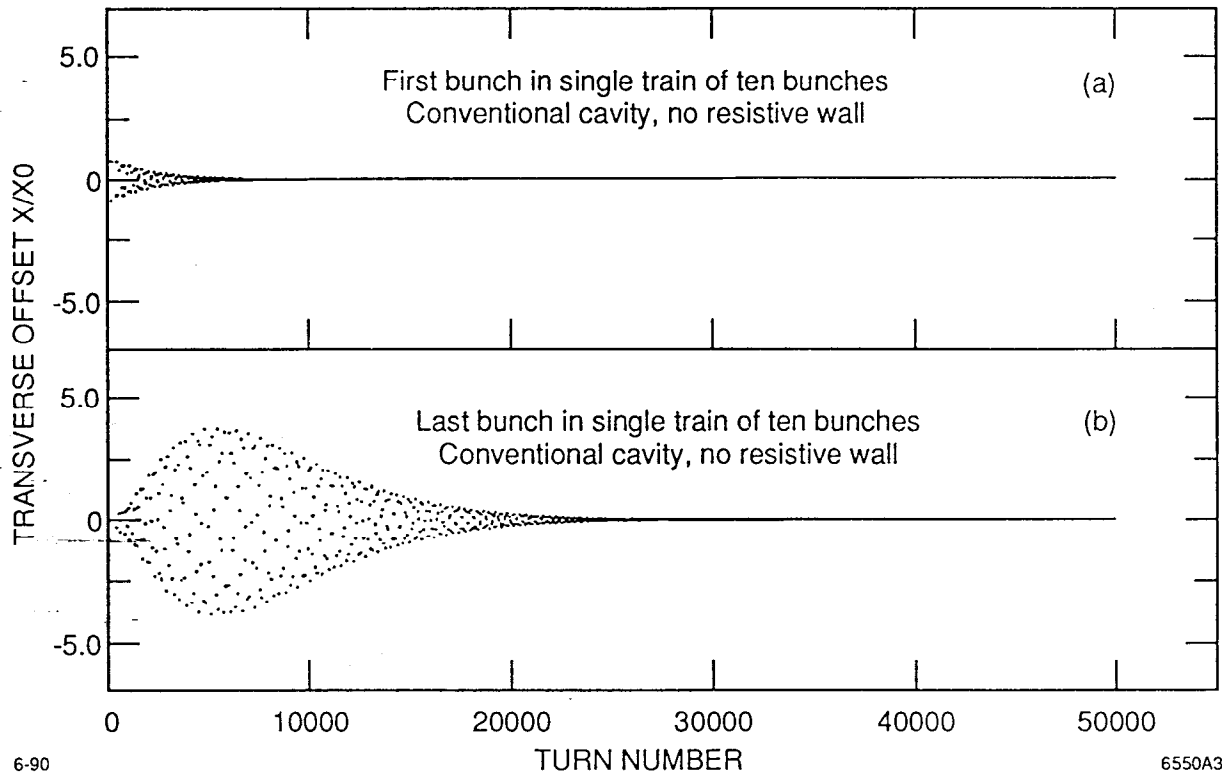


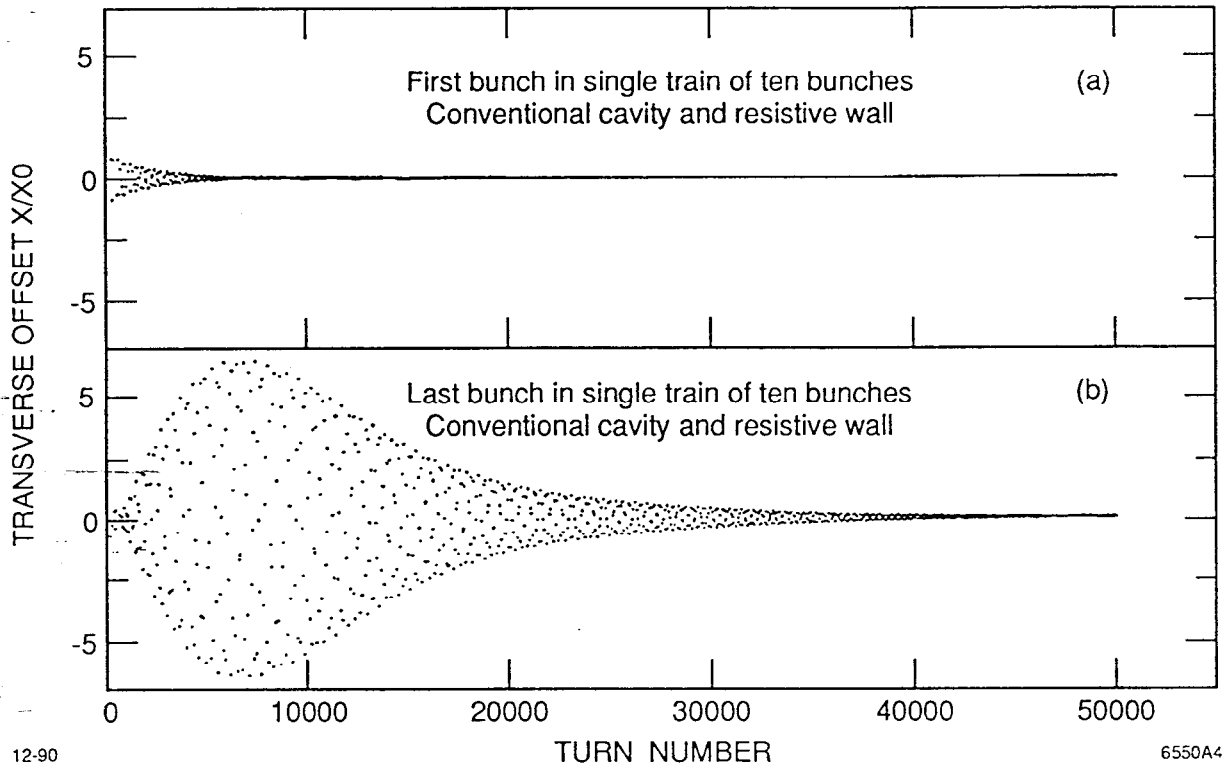
Fig. 1



6-90

6550A3

Fig. 2



12-90

6550A4

Fig. 3

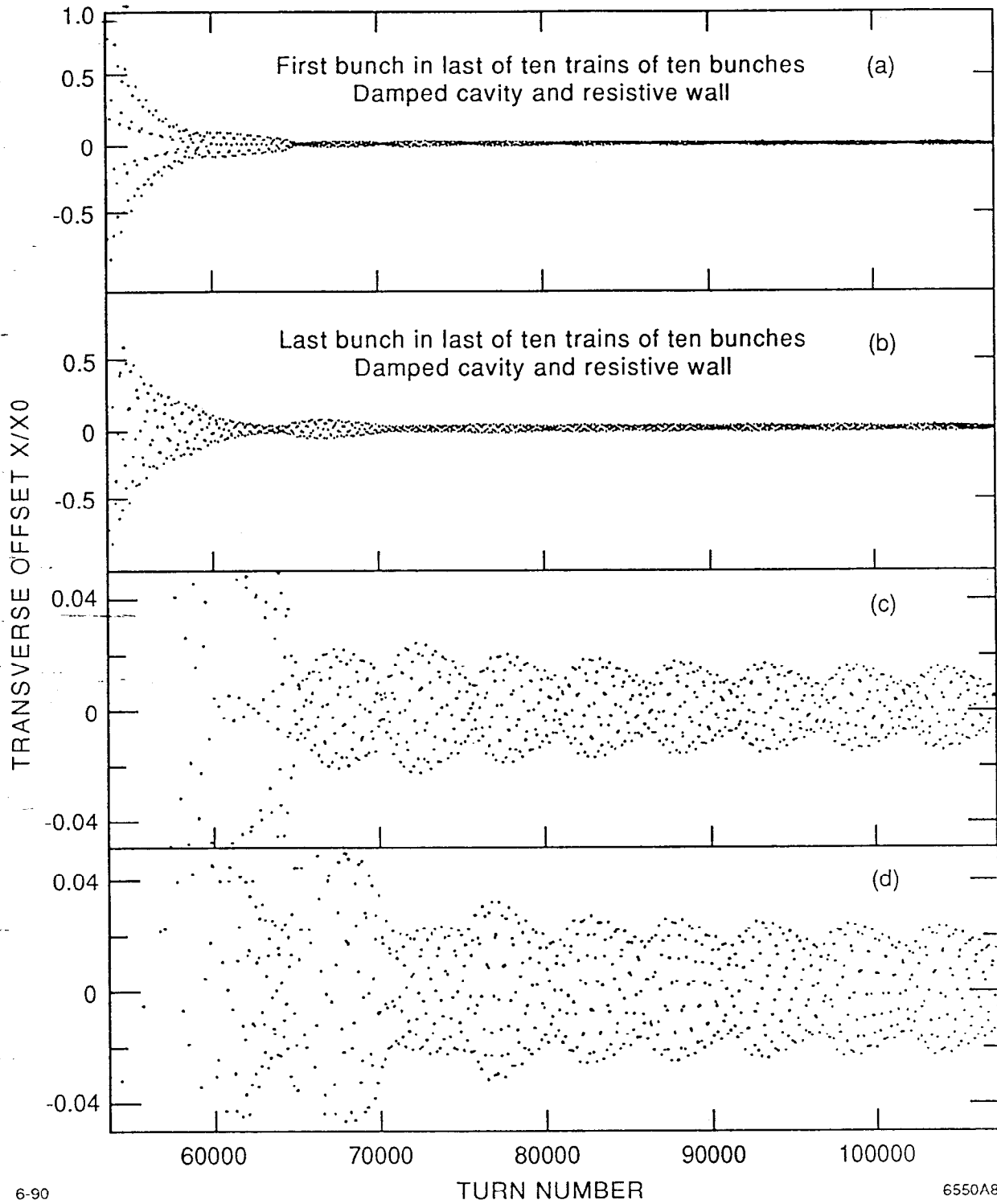


Fig. 4

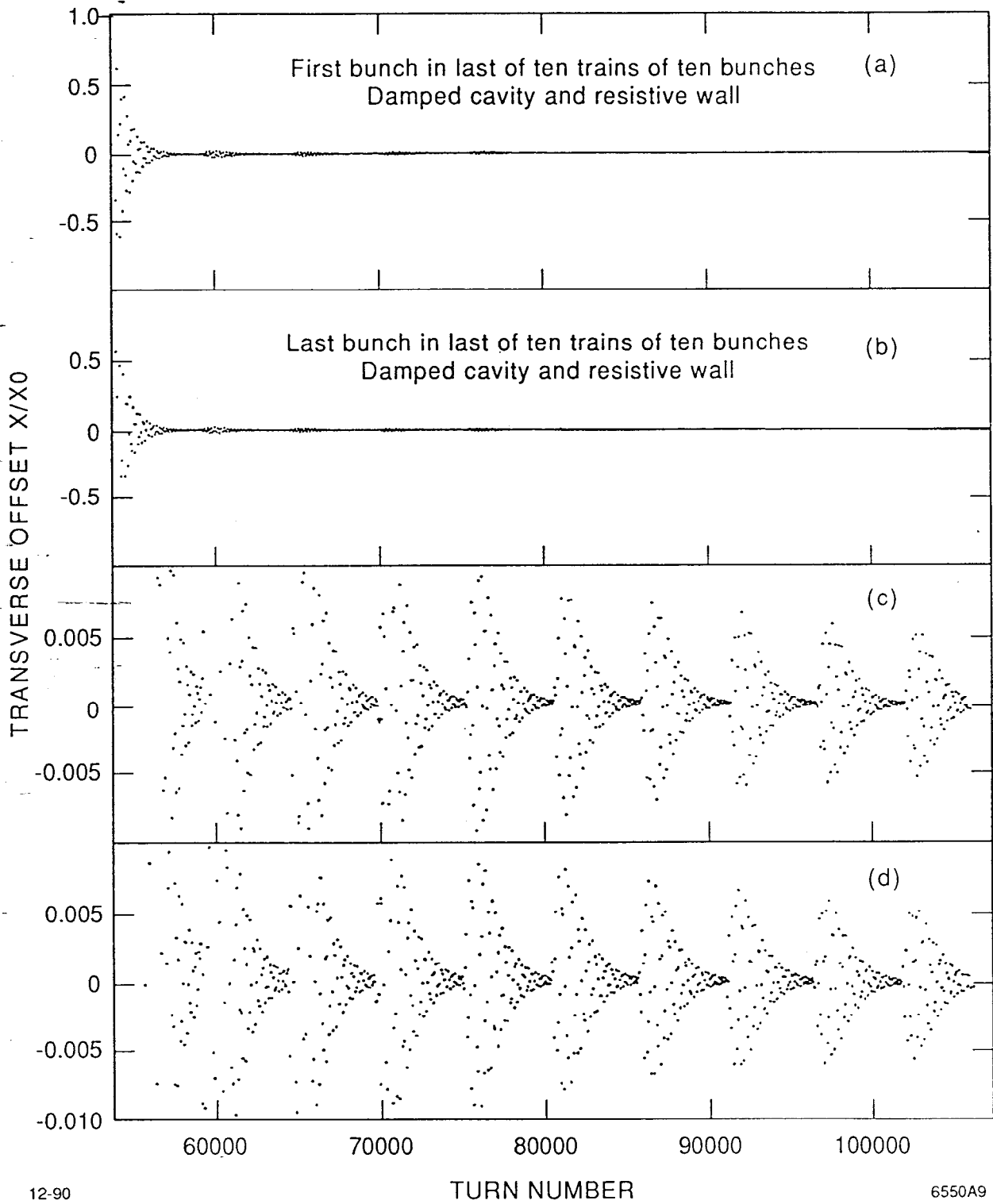


Fig. 5